INTERNAL BALLISTICS ANALYSIS FOR THE RAVEN PROPULSION SYSTEM

S. Dunn, J. French, and D. Coats*
E. Kathe, R. Dillon, S. Sopok, and M. Witherell†

* *Software and Engineering Associates, Inc., 1802 N. Carson Street, Suite 200, Carson City, NV, 89701-1230, www.seainc.com.*
† *US Army, TACOM-ARDEC, Benét Laboratories, Watervliet Arsenal, NY 12189-4050*

ABSTRACT

The recently proposed light Future Combat System (FCS) vehicles require a highly lethal cannon with greatly reduced recoil momentum. A novel approach to this problem was proposed by Kathe[1], which utilizes a **RA**refaction wa**VE** gu**N** (**RAVEN**) propulsion system to significantly reduce the recoil momentum and barrel heating. To accurately assess the effectiveness of this approach, a Navier-Stokes flow solver was developed to calculate the internal ballistics of this unconventional hybrid propulsion system. The results of the internal ballistics analysis for the current 120mm M256 firing an M829A2 Kinetic energy round indicated that the proposed system could theoretically reduce the recoil momentum by 75% and reduce the barrel heating by 50%[1].

INTRODUCTION

The **RAVEN** propulsion system may be considered a hybrid technology with features common to both closed-breech cannons and recoilless rifles. The basic principal behind this concept is derived from the fluid dynamic laws which state that a disturbance can not travel faster than the speed of sound in addition to the local velocity of the gases through which it propagates. Therefore, if the gases at the breech plate are allowed to vent to the atmosphere at the time when the projectile is approximately one-forth the way down the barrel, the resulting rarefaction wave will not reach the projectile until it exits. The resulting recoil forces will be significantly reduced due to both the elimination of the high-pressure acting on the breech plate and the momentum of the venting gases.

The validity of the concept was initially supported by simple one-dimensional calculations and approximations, which subsequently required more rigorous verification. Unfortunately, the tools required to validate the **RAVEN** concept did not exist, although there was an existing internal ballistics computer code which had most of the required capabilities. The **G**un **T**ube **B**oundary **L**ayer (**GTBL**) code was developed for Benét Laboratory in support of calculating thermochemical erosion in gun tubes. The **GTBL** code is a time accurate Navier-Stokes analysis used to calculate the fluid flow and heat transfer in gun barrels including the effects of a moving boundary, spatial mass addition, chemistry, and spatial compressibility. The code incorporates a feature that allows adjustable boundary conditions for each boundary node, which may vary with time, pressure, or any other defined variable.

DISCUSSION

The **G**un **T**ube **B**oundary **L**ayer (**GTBL**) Code was developed as a collaborative effort between Software and Engineering Associates Inc. and ROYA Inc in support of Benét Laboratories[2]. **GTBL** is an adaptation of an earlier **L**iquid **T**hrust **C**hamber **P**erformance (**LTCP**) code that implements a multispecies/multiphase Navier-Stokes flow solver using a fully implicit discretization scheme[3]. The left and right states of the inviscid fluxes for both phases are based on the Total Variation Diminishing (TVD) method. The Lax-Friedrichs and Van-Leer methods are implemented for the gaseous phase to calculate the total inviscid fluxes by combining the left and right states. Both schemes are second order accurate in space.

The **GTBL** code required the extension of the **LTCP** code to include time and position dependent mass addition to model the burning of the propellant grains, and the moving boundary condition of the base of the projectile. Due to the extremely high pressures and gas densities, local compressibility effects were included. The code also had to be time accurate. The analysis incorporated the mass addition and moving boundary conditions provided by the **NOVA**[4] interior ballistics code. This enabled the leveraging of this existing and well-calibrated interior ballistic code to effectively drive the **GTBL** code. This approach effectively de-couples the two-dimensional flow challenges associated with burning rates, propellant grain form functions, bore friction, projectile motion, etc. Also, integration of the detailed interior ballistics model into the **GTBL** code would result in extensive challenges that would require almost all-available resources, and thus was not undertaken. Therefore, the **GTBL** development was concentrated on the higher fidelity interior ballistic flow characteristics associated with the **RAVEN** analysis.

Although the **GTBL** code has the capability to evaluate fully kinetic chemistry, the following analysis employed equilibrium chemistry. This is justified because of the extremely high-pressure levels and the relatively long characteristic times. This assumption reduced computer run time by a factor of more than ten-fold, without appreciably changing the validity of the solution. The **C**ompressible **C**hemical **E**quilibrium and **T**ransport Property Program (**CCET 1.5™**)[5] was used to generate a Mollier Chart of equilibrium gas properties, including the compressibility term. These tables were subsequently used by the **GTBL** code to evaluate the fluid dynamic properties and their derivatives. The baseline **GTBL** code was validated by comparison to **NOVA** and associated data. Although there are several unresolved discrepancies (for example, the temperature at the base of the projectile for **NOVA** is approximately 1000° higher than the adiabatic flame temperature, while the corresponding temperature for **GTBL** is near the adiabatic flame temperature), the overall comparison was favorable.

Adding the capability for the gases to exhaust to the atmosphere at the breech plate at a prescribed time required a significant program modification. Although the ultimate goal is to model a complete nozzle attached to the breech plate, the scope of the study required a scaled down approach. It was decided to uncouple the solution, with the subsonic portion included within the **GTBL** code, and the supersonic nozzle portion as a subsequent stand-alone analysis. Thus, the boundary conditions at the breech plate were modified to allow subsonic flow exiting the chamber at a prescribed time. This approach approximated the subsonic entrance portion of a converging-diverging nozzle section. The opening process was simulated by continuously changing the subsonic area ratio from a very large area ratio to the final value of approximately 1.05. The resulting subsonic Mach Number boundary condition went from near zero to 0.70. Both a *fast (opening time of 0.1 ms)* and *slow (opening time of 1.0 ms)* opening scenario were analyzed, which simulate a burst disk and an inertial system, respectively.

ANALYSIS: 120mm M256/M829A2 GUN SYSTEM

A **CCET 1.5™** analysis was performed for the M829A2 propellant to generate a Mollier Chart, which was subsequently used as input to the **GTBL** code. This table provides gas and transport properties over a large range of temperatures and pressures. Dr. S. Sopok of Benét Laboratory performed a **NOVA** analysis for an ambient temperature firing of the 120mm M256/M829A2 gun system. The results of the **NOVA** run, which were used as input to the **GTBL** code, included geometry and gas production rates. The **GTBL** analysis was run with 25 radial nodes and 151 axial nodes, which was determined to yield the minimum acceptable accuracy. The grid structures at the initial and final times are shown in Figures 1 and 2, respectively. All computations assumed an adiabatic wall boundary condition, since a cold wall boundary condition requires a much finer radial node spacing resulting in significantly longer run times.

The nominal baseline case without venting was run from the start of ignition until 0.0180 seconds, which accounted for virtually all of the recoil momentum. At the time the projectile reached the muzzle exit plane, the moving boundary condition was changed to a non-moving extrapolative boundary condition, allowing flow to exit the barrel. In order to maintain acceptable accuracy, approximately 45,000 time steps were taken. Typical internal ballistic pressure and temperature contours are shown in Figures 3 and 4.

The earliest time at which the chamber of a gun could be vented without compromise can be computed from the output of the above non-venting case. The speed of sound including the effects of compressibility can be calculated using the **CCET 1.5™** code. This value can then be added to the local gas speed to determine the speed at which a rarefaction wave would travel. The rarefaction wave may be assumed at the muzzle exit plane, with the base of the projectile at shot exit. The wave front may then be back propagated through time using Euler's method. The results for the above case (ambient temperature firing of an M829A2 out of an M256) are shown in Figure 5. Based on the above analysis, a venting time of 0.0038 seconds was chosen.

The fast opening scenario, which simulates a burst disk, assumed that at 0.0038 seconds the vent was closed, while at 0.0039 seconds the vent was fully opened. The opening process was approximated by a cubic 'S' function, whereby the subsonic area ratio was 10,000 at the start of opening and 1.05 when fully opened. For purposes of comparison, the same grid structure was used for all cases, with approximately 10,000 more time steps than the non-venting case. Corresponding internal ballistic pressure and temperature contours for the fast venting scenario are shown in Figures 6 and 7.

The slow opening scenario, which simulates an inertial system, assumed that at 0.0038 seconds the vent was closed, while at 0.0048 seconds the vent was fully opened. The opening process employed the same function as the fast opening scenario. As with the fast venting scenario, the same grid structure was used, with approximately 12,000 more time steps than the non-venting case. Resulting internal ballistic pressure and temperature contours for the slow venting scenario are shown in Figures 8 and 9.

RESULTS: 120mm M256/M829A2 GUN SYSTEM

Since the gas production term was taken from **NOVA**, the results of the baseline scenario were compared with **NOVA** output as a merit of consistency. It should be noted that **NOVA** is a

one-dimensional Euler analysis, while **GTBL** is an axially symmetric Navier-Stokes analysis. Therefore, the following comparison is for the **GTBL** centerline solution. Figure 10 shows the comparison of the pressures at the breech plane and projectile base, and Figure 11 shows the comparison of the temperatures at the same locations. Both solutions show remarkable agreement for the breech pressure, while the projectile base pressures show some divergence. This could be attributed to the fact that at each time **NOVA** uses a global compressibility term, while **GTBL** utilizes a local compressibility function. The compressibility variation for the Breech plane and projectile base is shown in Figure 12. The temperature comparisons show a basic inconsistency, whereby the **NOVA** temperature at the projectile base is almost 1000°R higher than the adiabatic flame temperature of the propellant. Also, the **NOVA** temperature at the breech plane is almost 1000°R lower than the adiabatic flame temperature. The **GTBL** temperature solution appears to be consistent with the adiabatic flame temperature (approximately 6300°R), and no further attempt has been made to resolve these differences.

Figures 13 through 16 show the pressure and temperature histories at the centerline for the breech plane and projectile base for the baseline, slow, and fast venting scenarios. Figure 17 shows the projectile velocity for the baseline, slow, and fast venting scenarios, which indicates that the velocity degradation is minimal. The above analysis has verified that the breech plane can be vented while the projectile has traveled a short distance in the barrel without a loss in muzzle exit velocity.

SUMMARY: 120mm M256/M829A2 GUN SYSTEM

The reduction of the recoil impulse is due to three effects: 1) lower pressure in the chamber, 2) elimination of pressure force acting on the breech plate, and 3) anti-recoil force from the momentum of the exiting gas out a converging-diverging nozzle. The impact of the first two effects is calculated by the **GTBL** code. The net force resulting from the flow out a converging-diverging nozzle was calculated by an auxiliary code, which used the **GTBL** boundary outflow conditions as nozzle entrance conditions. From basic nozzle flow analysis, it can be shown that the most efficient configuration incorporates a very small subsonic entrance area ratio, and as large as possible exit area ratio. Therefore, the following analysis assumed that the fully opened subsonic entrance area ratio was 1.05, with exit area ratios of 5 and 50.

Figure 18 shows the recoil force and impulse for the baseline scenario. Figure 19 shows the mass outflow history for the fast opening scenario. Figures 20 and 21 show the fast opening recoil force and impulse for exit area ratios of 5 and 50, respectively. Figure 22 shows the mass outflow history for the slow opening scenario. Figures 23 and 24 show the slow opening recoil force and impulse for exit area ratios of 5 and 50, respectively. Figure 25 shows a comparison of the recoil impulse for the baseline, fast and slow opening scenarios. It can be seen that the fast opening scenario with an exit area ratio of 50 reduces the total recoil impulse by approximately 75 percent.

For purposes of comparison, the heat transfer in the barrel was calculated from the **GTBL** boundary layer edge conditions, using the analysis incorporated in **NOVA**. Figure 26 shows a comparison of the cumulative heat input into the barrel for the **NOVA** analysis, and the **GTBL** baseline, fast, and slow venting analysis. The fast opening scenario reduces the total heat load by approximately 50 percent.

CONCLUSIONS: 120mm M256/M829A2 GUN SYSTEM

The above Navier-Stokes internal ballistic analysis verified that the basic **RAVEN** propulsion system significantly reduces the recoil momentum and barrel heating. The reduction was greatest for a fast opening scenario, which simulates a burst disk. The slow opening scenario, which simulates an inertial system, is shown to be less efficient, but is still quite effective. Although the feasibility of the **RAVEN** propulsion system has been shown to be sound, implementation has not been completed to date, and could pose a formidable task.

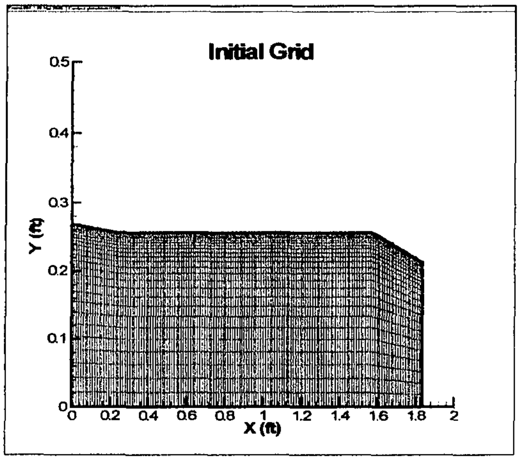

Figure 1. Initial Grid Structure

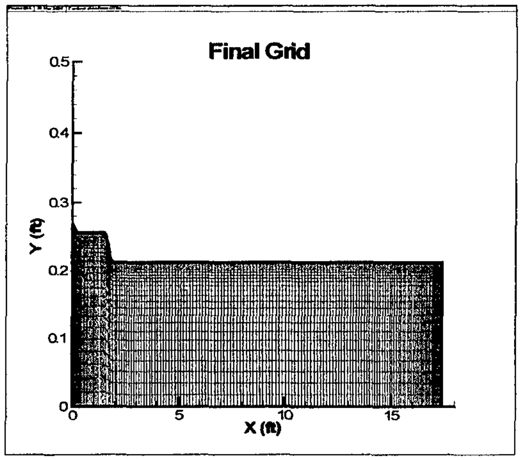

Figure 2. Final Grid Structure

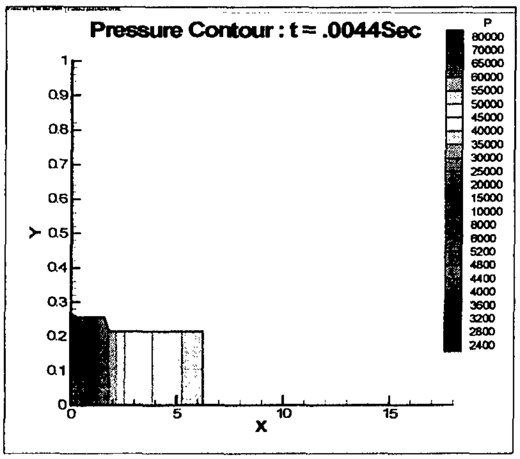

Figure 3. Pressure Contour for Baseline Scenario at t = .0044 Sec

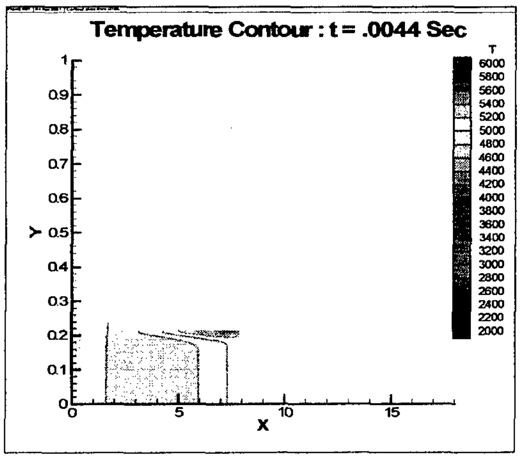

Figure 4. Temperature Contour for Baseline Scenario at t = .0044 Sec

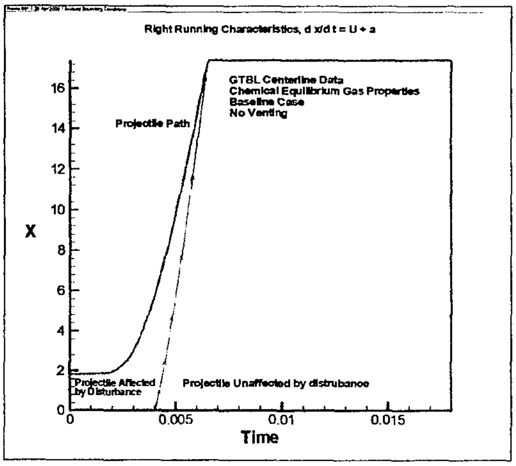

Figure 5. Propagation of Rarefaction Wave

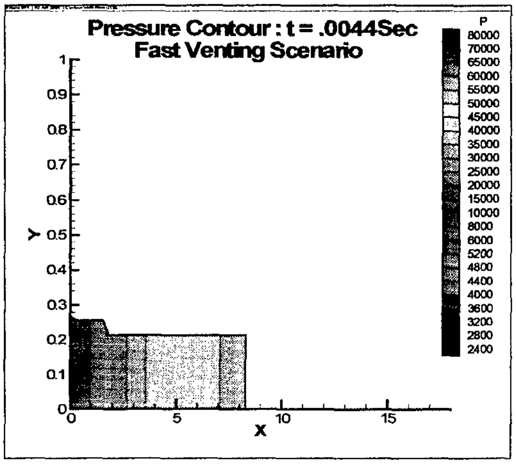

Figure 6. Pressure Contour for Fast Scenario at t = .0044 Sec

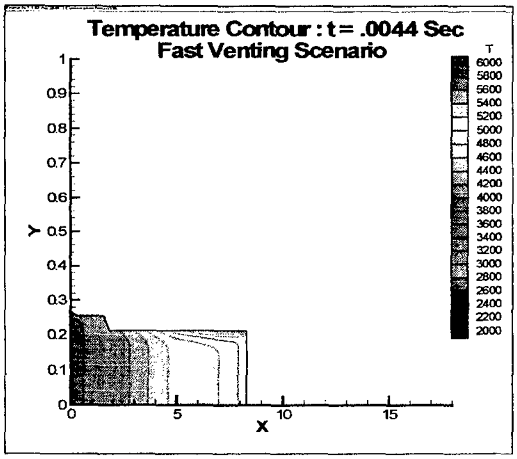

Figure 7. Temperature Contour for Fast Scenario at t = .0044 Sec

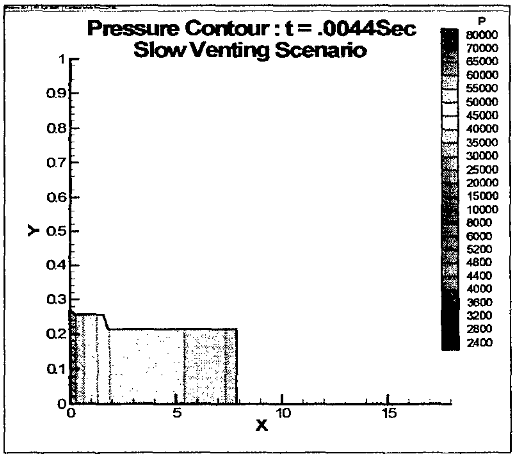

Figure 8. Pressure Contour for Slow Scenario at t = .0044 Sec

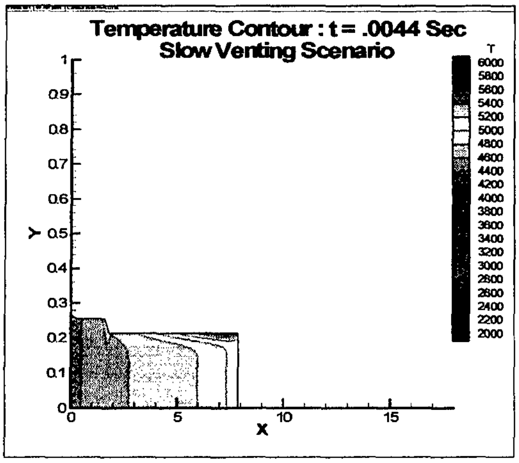

Figure 9. Temperature Contour for Slow Scenario at t = .0044 Sec

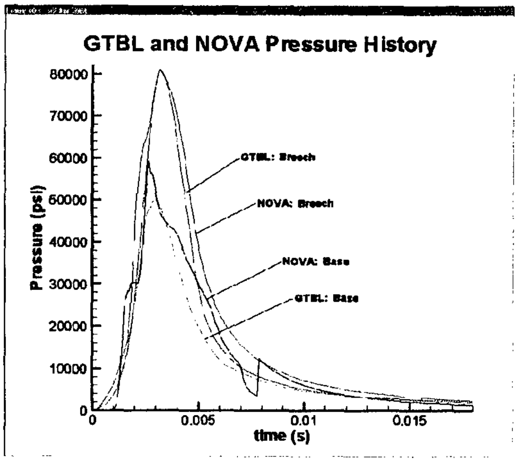

Figure 10. Comparison of GTBL and NOVA Pressure History at Breech and Projectile Base

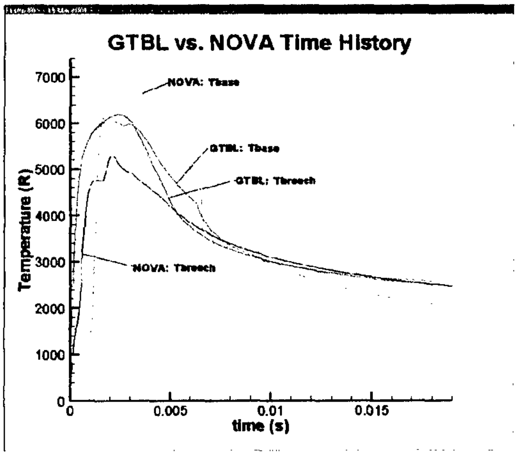

Figure 11. Comparison of GTBL and NOVA Temperature History at Breech and Projectile Base

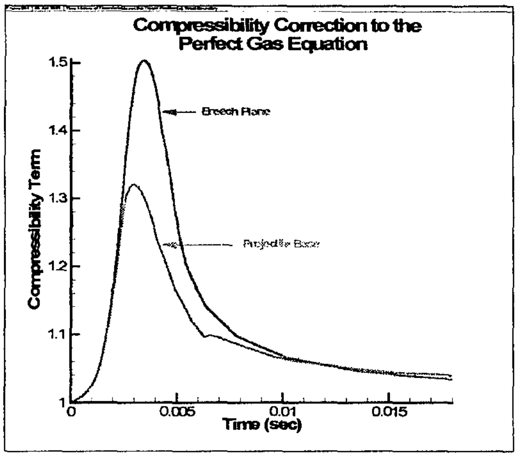

Figure 12. Compressibility Correction to the Perfect Gas Equation

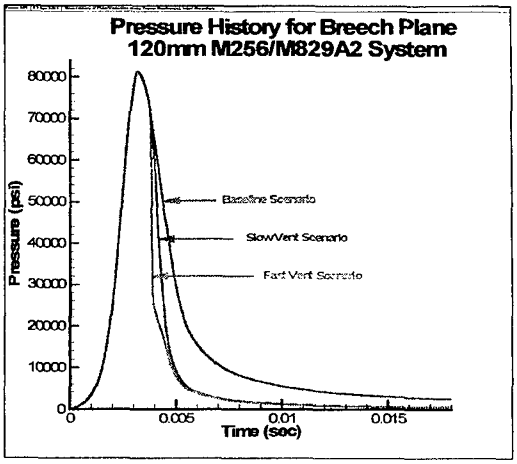

Figure 13. Pressure History for Breech Plane Centerline

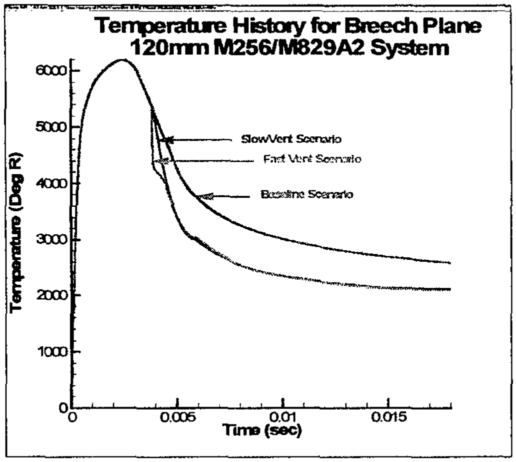

Figure 14. Temperature History for Breech Plane Centerline

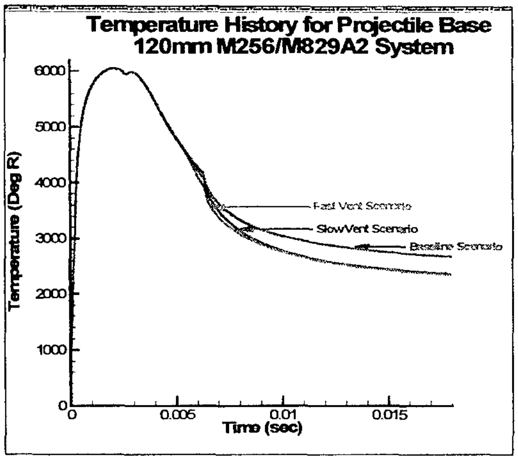

Figure 15. Pressure History for Projectile Base Centerline

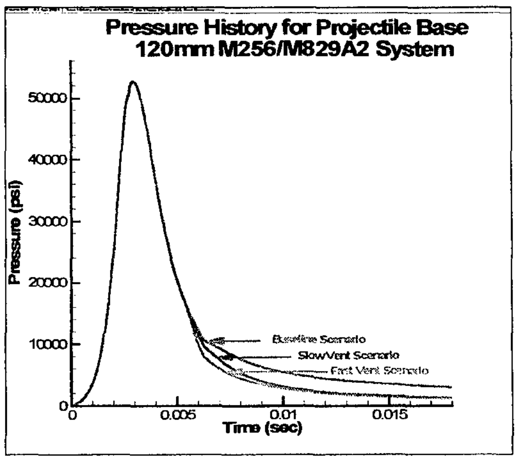

Figure 16. Temperature History for Projectile Base Centerline

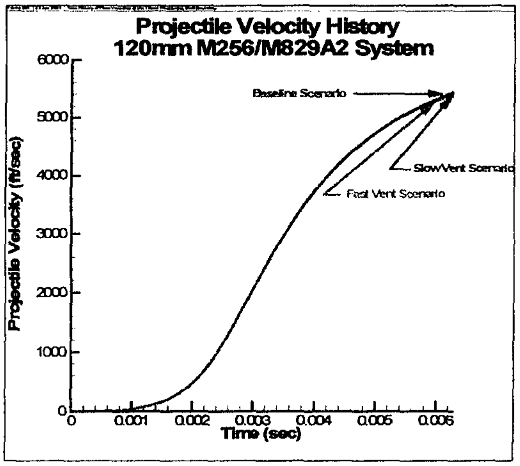

Figure 17. Projectile Velocity History

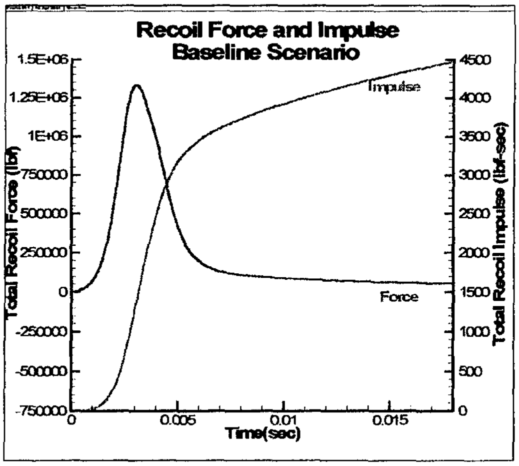

Figure 18. Recoil Force and Impulse for Baseline Scenario

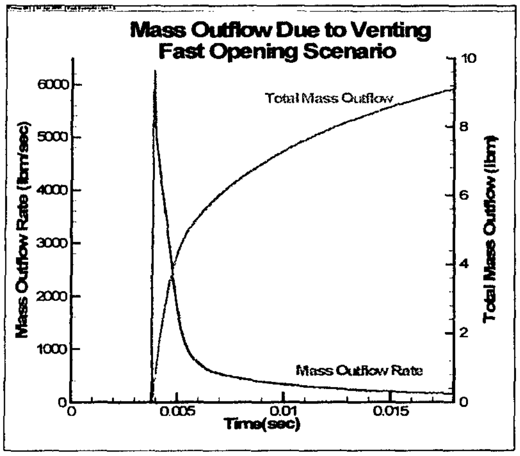

Figure 19. Mass Outflow Due to Venting for Fast Scenario

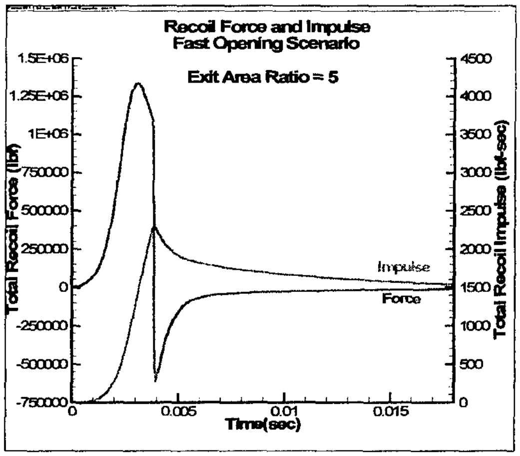

Figure 20. Recoil Force and Impulse for Fast Scenario, Eps=5

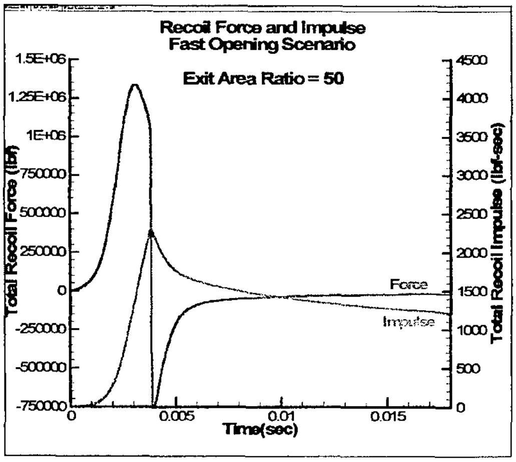

Figure 21. Recoil Force and Impulse for Fast Scenario, Eps=50

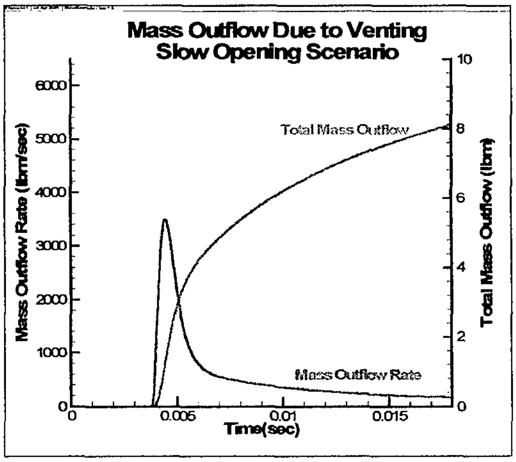

Figure 22. Mass Outflow Due to Venting for Slow Scenario

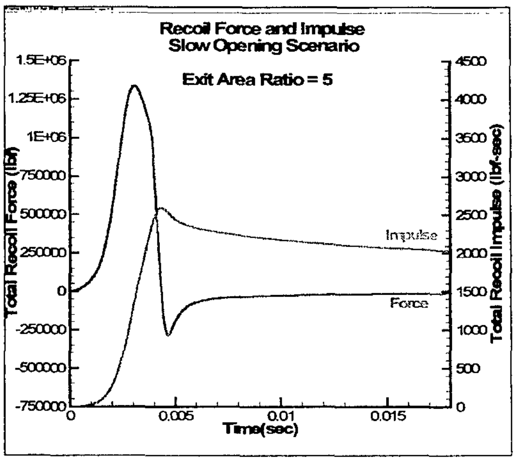

Figure 23. Recoil Force and Impulse for Slow Scenario, Eps=5

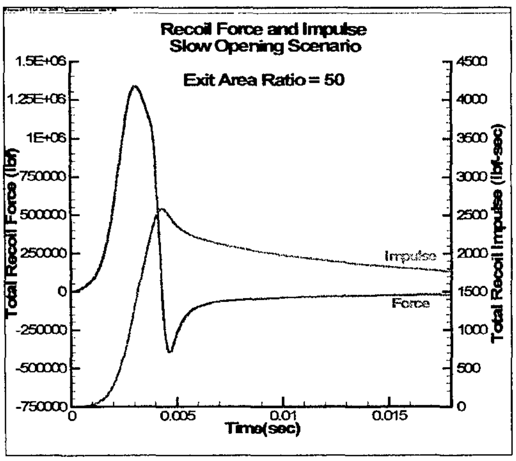

Figure 24. Recoil Force and Impulse for Slow Scenario, Eps=50

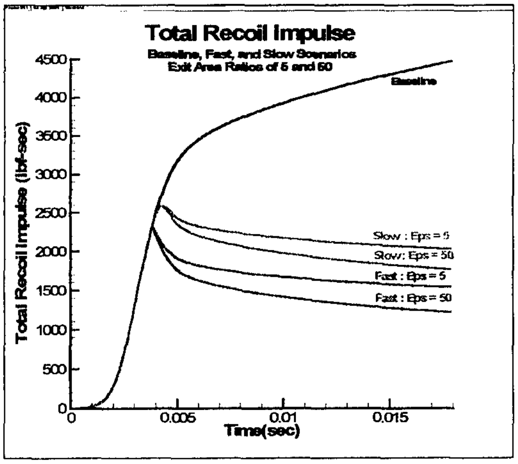

Figure 25. Total Recoil for Baseline, Slow, and Fast Scenarios

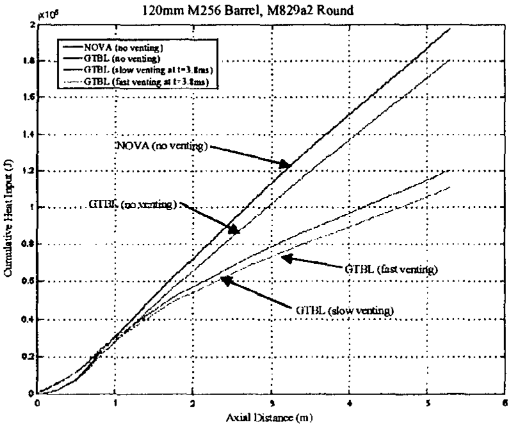

Figure 26. Effects of Venting on Barrel Heat Transfer

REFERENCES

1 Kathe, E., Dillon, R., Sopok, S., and Witherell, M., "Sonic Rarefaction Wave Low Recoil Gun," AIAA Paper Number AIAA-2001-0743, presented in Reno, NV, January 2001.

2 Navaz and Dunn, "A Computer Model for Gun Barrel Flow Analysis: The Gun Tube Boundary Layer Code (GTBL)," Final Report, Software and Engineering Associates, Inc., Carson City, NV, September, 1999

3 Navaz and Dang, "LTCP: Liquid Thrust Chamber Performance Computer Code," NASA Contract NAS 8-38798, Physical Research, Inc. Irvine CA, November, 1992

4 Gough, P., "The XNOVAKTC Code," U.S. Army BRL-CR-627, Paul Gough Associates, Portsmouth, NH, 1990.

5 Dunn, S., Coats, D., and Sopok, S., "A New Chemical Equilibrium Code with Compressibility Effects," Proceedings of the 33rd JANNAF Combustion Meeting, Monterey, CA, October 1996.